Optimization for the Train Plan with Flexible Train Composition Considering Carbon Emission

Changfeng Zhu,Xianen Yang,Zongfang Wang,Jinghao Fang,Jie Wang,and Linna Cheng

***Abstract*—Running trains with different train compositions on the metro line is one of the effective ways to solve the problem of mismatching between transportation capacity and passenger demand. In this regard, a train plan with flexible train composition (TPFTC) is proposed, and the metric of carbon emission during metro operation is analyzed. A multi-objective programming model is established under the constraints of the maximum full load rate of the train and the number of operating vehicles. The decision variables are the location of two turnaround stations and the operation frequencies. In addition, the objective functions consider not only minimizing the travel cost of passengers and the metro corporate operating costs, but also minimizing carbon emissions during metro operation. Based on the proposed model, an improved quantum genetic algorithm (IQGA) is designed to solve the mathematical model. Finally, the rationality of the model is verified through a case study. The results indicate that compared with the traditional train plan(TTP) with fixed train composition, TPFTC can significantly increase the average full load rate of the line without reducing the service level, and it plays a significant role in energy saving and emission reduction for the metro operator. In addition, the higher the operation frequencies, the more pronounced the advantages of TPFTC. The study concluded that the larger the limit value of the maximum full load rate, the more pronounced the effect of energy saving and emission reduction. And the flexible selection of unit trains is conducive to energy saving and emission reduction.**

***Index Terms*—Train Plan, Flexible Train Composition, Carbon Emission, Quantum Genetic Algorithm(QGA)**

Manuscript received October 18, 2022; revised March 20, 2023.

This work was supported in part by the National Natural Science Foundation of China (No.72161024) and "Double-First Class" Major Research Programs, Educational Department of Gansu Province (No.GSSYLXM-04).

Changfeng Zhu is a professor at School of Traffic and Transportation, Lanzhou Jiaotong University, Lanzhou 730070, China. (e-mail: cfzhu003@163. com).

Xianen Yang is a postgraduate student at School of Traffic and Transportation, Lanzhou Jiaotong University, Lanzhou 730070, China. (Corresponding author, phone: +86 13993329402, e-mail: xianenyang0623@163. com).

Zongfang Wang is a postgraduate student at School of Traffic and Transportation, Lanzhou Jiaotong University, Lanzhou 730070, China. (e-mail: 1781116144@qq.com).

Jinghao Fang is a doctoral candidate at School of Traffic and Transportation, Lanzhou Jiaotong University, Lanzhou 730070, China. (e-mail: fangjin_hao@163.com).

Jie Wang is a doctoral candidate at School of Traffic and Transportation, Lanzhou Jiaotong University, Lanzhou 730070, China. (e-mail: 1009696615@qq.com).

Linna Cheng is a doctoral candidate at School of Traffic and Transportation, Lanzhou Jiaotong University, Lanzhou 730070, China. (e-mail: chenglinnajiao@126. com).

I. INTRODUCTION

CARBON dioxide emission related to human economic activities will lead to unstable changes in the global climate [1]. Today, carbon emission has become a global problem. According to the International Energy Agency (IEA) data, 23% of global energy-related carbon emission comes from the transport sector, which will grow to 41% by 2030 [2]. Stations and trains will directly or indirectly generate a large amount of carbon emission in the process of metro operation. The energy consumption generated in the metro operation accounts for about 40% of the total energy consumption [3].

Due to the unbalanced spatial distribution of passenger demand on metro lines, the TTP has insufficient transportation capacity in the line section with high passenger demand, which causes a waste of transportation capacity in the section with low passenger demand [4]. Moreover, the train operation without passengers will increase the carbon emission in the metro operation. The flexible train composition [5] refers to the flexible adjustment of train composition lengths by coupling and uncoupling trains with different composition length during train operation under the condition of ensuring operation safety. It aims to run trains with different compositions in different sections of the line according to different passenger flow demands to make the transportation capacity and passenger demand optimally match. The carbon emission in the metro operation can be reduced.

The train plan aims to optimize the frequencies of the train services, turnaround plan, and train stopping strategy in the process of train operation according to the demand of metro passenger flow [6]. At present, many scholars have done rich researches on the train plan. Among them, an optimization model for the optimal frequencies of urban rail transit was established in [7] by minimizing the number of train operating periods and maximizing the full load rate of the train. An optimization model of an unbalanced train operation plan in a congested environment was constructed by [8]. A bilevel programming mode was proposed in [9], which took the train tracking interval time as the decision variable and reduced the travel time as the optimization goal. Reference [10] optimized the train plan according to the dynamic changes in passenger flow and prepared a timetable with variable departure intervals. The above scholars have done fundamental researches on the train plan. However, they were all studied under fixed train composition, and the flexible train composition was not considered.

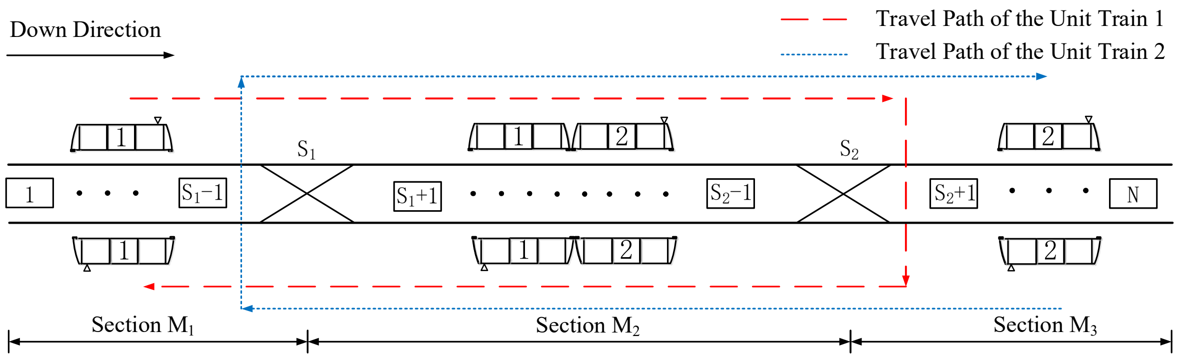

Fig.1. Schematic diagram of TPFTC

Therefore, in recent years, some scholars have done a series of studies on the train plan considering flexible train composition. References [11][12][13] divided the day into different periods, and ran trains with different operation frequencies and a number of trains in each period, in order to optimally match the transportation capacity and transportation volume in different periods. Skip-stop operation is considered by [14] based on different train compositions, and a model was built comprehensively considering passenger interests, business interests, and robustness to optimize the timetable. Considering the interests of operators and passengers, a nonlinear integer programming model with two sub-models of train service design was developed by [15] to determine the turnaround stations, train compositions, and operation frequencies. The optimization model of the multiple service routes and multiple train compositions train plan was established by [16][17],which taking the minimum operating cost and passenger waiting time as the optimization goal, and taking the position of the turnaround stations, train composition and operation frequencies as the decision variables. Considering the trains of different compositions under the cross-line operation mode, a bilevel programming model was established by [18] to determine the operation frequencies, turnaround stations and train composition numbers with the optimization goal of maximizing the passenger travel time savings, maximizing the revenue of the metro operation enterprise, and maximizing the balance of the train's full load rate. In the case of the uneven spatial distribution of cross-sectional passenger flow, the optimization model of a virtual-coupling-orientated train plan based on full-length and short-turn routing was constructed by [19] to minimize the train operating mileage.

In addition, references [20][21] studied train timetabling and rolling stock circulation planning considering flexible train composition for different compositions of the train running up and down under the background of unbalanced passenger demand. According to passenger demand, [6][22] considered running multiple train compositions on metro lines to solve the problem of mismatch between transportation capacity and transportation volume, and studied the related issues of train timetabling and rolling stock circulation planning.

The above studies have done a detailed study of the train plan with flexible train composition. However, most of the studies considered optimizing the travel cost of passengers and metro corporate operating costs. However, more consideration should have been given to reducing carbon emission in the operation process.

Based on the above analysis, minimizing the travel cost of passengers and metro corporate operating costs, and considering the minimum carbon emission in the operation process, a multi-objective programming model is established with the operation frequencies and turnaround station locations as the decision variables. An improved quantum genetic algorithm (IQGA) is designed to solve this model.

II. Problem Description

Suppose a metro line is L long, including N stations, the spatial distribution of cross-section passenger flow is atrophic distribution at both ends [23], it means the cross-section passenger flow at both ends of the line is small, and the passenger flow of the middle section is large. Trains operating on the line are divided into unit trains and reconnection trains. Unit trains refer to the smallest unit train set with operating conditions. This paper uses the train with three vehicles as a unit train. The reconnection train is coupled with two unit trains through coupling operation on the line. The TPFTC is shown in Fig.1.

As can be seen from Fig.1, the stations are numbered 1 to N from left to right on the line. The set of stations is $n=\{ n_i \,|\, i=1, 2,\dots, N\}$, represents the OD volume of passenger flow between station i and station j in direction ϕ, ϕ values are 1 and 2, where 1 represents the down direction and 2 represents the up direction. For the convenience of description, according to the number of the train composition in the operation section, the line is divided into three different sections with the turnaround stations s_1 and s_2 as the dividing points, which are denoted as M_1, M_2 and M_3 respectively. Among them, sections M_1 and M_3 have a small passenger flow and run unit trains, and section M_2 has a large passenger flow and runs reconnection trains. The operation frequencies f of the up and down trains is a fixed value during the research period so that the train plan can be expressed as $\Omega=\{f, s_1, s_2\}$. The specific operation process of the train in the section with flexible train composition is shown in Fig.2.

As shown in Fig.2, at time t_1, the reconnection train reconnected by unit train 1 and unit train 3 at station s_1 arrives at the turnaround station s_2. During the period of t_1-t_2, the reconnected train is uncoupled into two unit trains, of which unit train 1 returns to station N, and after the turnaround operation, unit train 3 reconnects with the unit train 4 as a reconnection train during the period t_1-t_3. It starts in the upward direction at time t_4 and arrives at the turnaround station s_1 at time t_5. During the period t_5-t_6, the reconnection train is uncoupled into two unit trains, of which unit train 3 returns to station N, and unit train 4 couples with unit train 5 during the period t_7-t_8 to couple to a reconnection train, which is sent in the downward direction at time t_8. Thus forming a cycle.

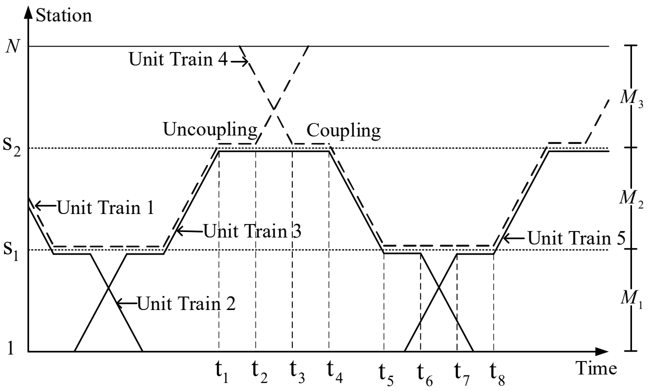

Fig.2. Schematic diagram for train plan with flexible train composition

III. Model Construction

With the background that cross-section passenger flow is spatially distributed in an atrophic distribution at both ends, trains of different compositions are operated in the course of train operation organization. There are two advantages. On the one hand, it avoids transportation capacity waste and reduces the metro operator's cost. On the other hand, based on energy saving and emission reduction, the operation frequencies are shortened and the service quality of the metro operator is improved. Based on this, we establish a multi-objective programming model to optimize the train plan to minimize passengers' travel costs, metro corporate operating costs, and carbon emissions for the metro operator. The model assumptions are as follows:

a. The OD passenger flow during the study period is known and the passenger arrivals obey a uniform distribution.

b. The train runs in the station-stop mode and the various facilities of the line and stations meet the conditions for online coupling and uncoupling operations.

A. Objective Function

A.1. Travel Cost of Passengers

On the one hand, the travel time of passengers should be considered, on the other hand, the comfort of passengers during the journey should be considered. We measure the comfort of passengers through the congestion costs.

Passenger transit time generally comprises inbound, outbound, waiting, and travel time. Since we assume that trains operate in a stop-station mode and travel at the same speed for different compositions of trains, the travel time of passengers is same and the time of entering and exiting the station is same, so only the waiting time of passengers is analysed. The research shows when the arrival of passengers is subject to a uniform distribution, the average waiting time of passengers is equal to half of the departure interval [10]. The average waiting time t_w for a passenger can be calculated by (1).

$$t_w = \frac{60\alpha}{f} \tag{1}$$

Where, α is the passenger waiting time parameter and takes the value 0.5 when passenger arrivals follow a uniform distribution.

The OD passenger flow q_{ij}^{ϕ} during the study period is known, so the cross-section passenger flow $\mu_{i,i+1}^{\phi}$ can be calculated by (2).

$$\mu_{i,i+1}^{\phi} = \sum_{i'=j+1}^{N}\sum_{i'=1}^{i} q_{ij}^{\phi} \tag{2}$$

Where, $i, j, i', j' \in n$.

As the train plan in this paper has different train composition plans within different sections, the congestion costs are studied by section.

In the sections M_1 and M_3, the full load rate of the train $\eta_{i,i+1}^{\phi}$ can be calculated by (3).

$$\eta_{i,i+1}^{\phi} = \frac{\mu_{i,i+1}^{\phi}}{fQ} \tag{3}$$

Where, $i \in \{1,2,...,s_1\} \cup \{s_2, s_{2+1},...,N\}$;Q represents the train capacity of the unit train, people/unit.

In the section M_2, the full load rate of the train $\eta_{i,i+1}^{\phi}$ can be calculated by (4).

$$\eta_{i,i+1}^{\phi} = \frac{\mu_{i,i+1}^{\phi}}{2fQ} \tag{4}$$

Where, $i \in \{s_1, s_1+1,...,s_2\}$.

Reference [24] shows the congestion cost is a function of the full load rate of the train, expressed as (5).

$$f(\eta_{i,i+1}^{\phi}) = \begin{cases} 0 & \eta_{i,i+1}^{\phi} \le 1 \\ 0.15(\eta_{i,i+1}^{\phi})^4 & \eta_{i,i+1}^{\phi} > 1 \end{cases} \tag{5}$$

Where, 0.15 and 4 are dimensionless empirical parameters of passenger congestion cost [24].

To sum up, converting the waiting time of passengers into the monetary cost of waiting time, combined with the congestion costs, the total travel cost of passengers C_1 can be calculated by (6).

$$\begin{aligned} \min C_1 = & \sum_{\phi=1}^{2}\sum_{j=1}^{N}\sum_{i=1}^{N}\frac{\beta q_{ij}^{\phi} t_w}{60} + \sum_{\phi=1}^{2}\sum_{i=1}^{s_1-1} f(\eta_{i,i+1}^{\phi}) \times \mu_{i,i+1}^{\phi} \\ & + \sum_{\phi=1}^{2}\sum_{i=s_1}^{s2-1} f(\eta_{i,i+1}^{\phi}) \times \mu_{i,i+1}^{\phi} + \sum_{\phi=1}^{2}\sum_{i=s_2}^{N-1} f(\eta_{i,i+1}^{\phi}) \times \mu_{i,i+1}^{\phi} \end{aligned} \tag{6}$$

Where, β represents the average time value of a passenger, yuan/h.

A.2. Carbon Emission

Part of the electricity consumption generated during the operation of the metro comes from thermal power generation. Therefore, we calculate the quality of coal combustion through the ratio of rail transit power consumption and thermal power generation to measure carbon emission. According to China's National Energy Statistics Report data, it takes about 345g of standard coal to generate 1kW·h of electricity. The combustion value of standard coal is 29.3MJ/kg, and the emission coefficient of raw coal is 94600kg/TJ (calculated as CO_2). According to [25], urban rail transit carbon emission = power consumption during operation period × thermal power generation ratio γ × 0.345 kg×29.3MJ/kg×94600kg/TJ.

The carbon emission in the metro operation is mainly divided into the fixed energy consumption of the station and the energy consumption that changes during the train operation. Among them, the fixed energy consumption of the station is mainly caused by the energy consumption of air conditioners, escalators, lighting and other equipment. The fixed energy consumption does not change with the change in the train plan. Therefore, we aim to minimize the variable energy consumption generated during train operation, including the energy consumption of on-board equipment and traction energy.

a. The energy consumption of on-board equipment

In addition to traction energy consumption, it is mainly the air conditioning, signal system, lighting, and other equipment that generate power consumption during train operation. According to [25], the electrical power of air conditioning, lighting, and signal equipment on trains is calculated by (7),(8),and(9).

$$p_1 = n_1 \times n_c \times 40 \tag{7}$$

$$p_2 = s_c \times 2 \times |T_i - T_o| \times 3 \times n_c \tag{8}$$

$$p_3 = n_c \times 2 \times 230 \tag{9}$$

Where, p_1 represents the electrical power of the train lighting, w. n_1 represents the number of lamps in a single vehicle, unit. n_c represents the number of vehicles, unit. p_2 represents the electrical power of the train ventilation and air conditioning, w.s_c represents the surface area inside the vehicle, m^2.T_i and T_o represent the temperature inside and outside the vehicle, ℃. p_3 represents the electrical power of the train signalling system, w.

The above analysis shows that the carbon emission from on-board equipment such as train air-conditioning, lighting, and signalling is calculated by (10).

$$c_1 = 2 \times (p_1 + p_2 + p_3) \times f \times \left(\frac{\sum_{i=1}^{s_2-1} s_{i,i+1} + \sum_{i=s_1}^{N-1} s_{i,i+1}}{v}\right) \times \gamma \times 0.345 \times 29.3 \times 0.0946 \tag{10}$$

Where, $s_{i,i+1}$ represents the distance between stations i and $i+1$ in the district, m; v represents the average train speed, km/h.

b. Traction energy

Considering the conversion relationship of energy during train operation, according to [26], the traction energy consumption is calculated from the perspective of traction work, which is mainly used to overcome resistance work, increase the kinetic energy of the train and overcome the gravitational potential energy difference.

Considering the comprehensive consideration of up and down energy consumption in this paper, therefore, we assume that the line as a whole is flat and do not consider the effect of gravity work. Moreover, the train has been subject to the role of resistance in the whole interval running process. In the calculation of resistance work, the train in the whole interval is simplified as from the starting station to the end of the station at a speed of v uniform motion, the train running process of the unit basic resistance w_0 is calculated as (11).

$$w_0 = A + Bv + Cv^2 \tag{11}$$

Where, A,B,and C are the empirical coefficient of basic resistance (The values are 2.4, 0.014 and 0.001293 respectively).

Studies have shown that passenger flow impacts the energy consumption of trains. When passenger flow increases 30%, the energy consumption of train traction increases 5.7% [27]. Therefore, it is necessary to determine the traction quality of the train by taking into account both the deadweight and the cross-sectional passenger flow. The train traction mass $M_{i,i+1}^{\phi}$ is calculated for each section as (12) and (13). In the flexible train composition described in this paper, the work done by trains overcoming resistance during the study period E_r can be calculated as (14).

$$M_{i,i+1}^{\phi} = m_1 + m_2 \times \frac{q_{ij}^{\phi}}{f} \tag{12}$$

$$M_{i,i+1}^{\phi} = 2m_1 + m_2 \times \frac{q_{ij}^{\phi}}{f} \tag{13}$$

$$E_r = \sum_{\phi=1}^{2} \sum_{i=1}^{N-1} w_0 M_{I,I+1}^{\phi} g s_{i,i+1} \tag{14}$$

Where, (12) represents the section traction quality of the unit train sections M_1 and M_3. (13) represents section traction quality of the reconnecting composition section M_2.m_1 represents the quality of the unit train, kg.m_2 represents the quality of a passenger, kg. g represents gravitational acceleration, m/s^2.

The distance between adjacent subway stations is small, and there are generally four operating conditions during the operation of trains at two adjacent stations as shown in Fig.3(a): traction, cruising, inert working, and braking conditions. Since calculating the work done by the traction force from the kinetic energy perspective, the actual operating process is simplified to the process shown in Fig. 3(b).

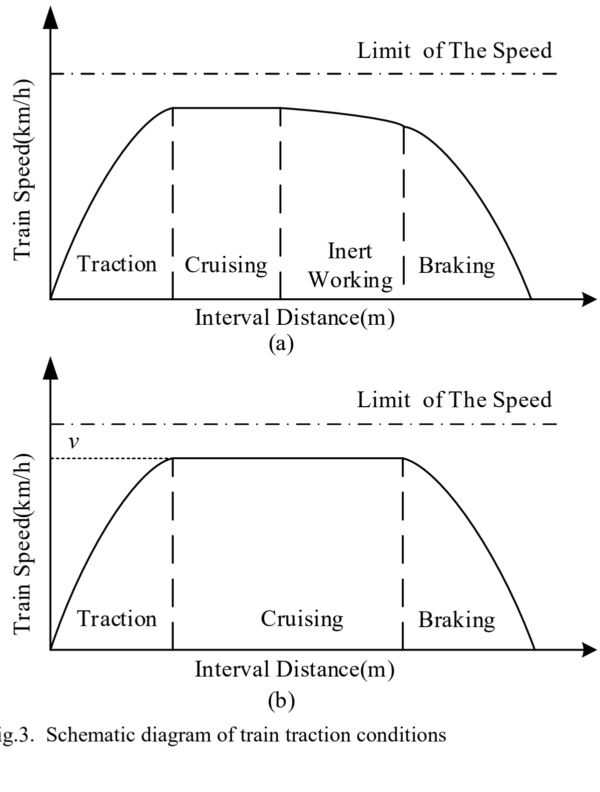

Fig.3. Schematic diagram of train traction conditions

As shown in Fig.3(b), the train undergoes three processes of acceleration, uniformity, and deceleration during each interval of operation, and the work done by the traction force is mainly to increase the kinetic energy of the train, which increases during the process of increasing the speed of the train from 0 to the maximum operating speed v_{max}, so the work done by the traction force in each interval $E_{i,i+1}$ is calculated by (15). In the flexible train composition described in this paper, the work done by the train to overcome the resistance during the study period E_t is calculated by (16).

$$E_{i,i+1}=\frac{1}{2}M_{i,i+1}^{\phi}v_{\max}^{2} \tag{15}$$

$$E_{t}=\sum_{\phi=1}^{2}\sum_{i=1}^{N-1}\frac{1}{2}M_{i,i+1}^{\phi}v_{\max}^{2} \tag{16}$$

Therefore, the carbon emission caused by the traction energy consumption of metro during the study period c_2 is expressed as (17). The objective function for minimizing the carbon emission of the metro can be calculated as (18).

$$c_2=(E_r+E_t)\times f\times\gamma\times 0.345\times 29.3\times 0.0946 \tag{17}$$

$$\min C_2=c_1+c_2 \tag{18}$$

A.3. Metro Corporate Operating Costs

The metro corporate operating costs usually consist of fixed costs and variable costs. The fixed costs are mainly the vehicle allocation costs, while the variable costs depend on the total kilometres travelled by the train. In addition, considering the online coupling and uncoupling operation of trains, the cost of coupling and uncoupling operation w_5 is considered in the variable cost. w_5 is related to the operation frequencies f, and the single coupling and uncoupling cost is assumed to be c_5,thus $w_5=2f\,c_5$.

As trains have a specific time limit for running, in order to better measure the vehicle allocation cost during train operation, the vehicle allocation cost is considered to be evenly spread to each hour of train operation [28].The train acquisition cost w_1 can be calculated according to (19). Since in the train plan proposed in the text, the unit train sent in the up and down directions return to the departure station after the turnaround stations s_1 and s_2, the number of vehicles N_y in operation can be calculated according to (20). The train operating cost w_2 is the product of the train operating cost per kilometre and the kilometres travelled by the train, which can be calculated according to (21). Therefore, the objective function of minimising the metro corporate operating costs can be calculated according to (22).

$$w_1=\frac{c_3\times N_y}{T_y} \tag{19}$$

$$N_y=\frac{2\times f}{3600}\left(\sum_{i=1}^{s_2-1}t_{i,i+1}+\sum_{i=1}^{s_2}t_{i,s}+\sum_{i=s_1}^{N}t_{i,i+1}+\sum_{i=s_1}^{N-1}t_{i,s}+2\mathrm{t}_z\right) \tag{20}$$

$$w_2=2\times c_4\times f\times\left(\sum_{i=1}^{s_2-1}s_{i,i+1}+\sum_{i=s_1}^{N-1}s_{i,i+1}\right) \tag{21}$$

$$\min C_3=w_1+w_2+w_5 \tag{22}$$

Where, c_3 represents the unit train acquisition cost, yuan/ unit. T_y represents the number of hours converted from train service life, h. $t_{i,i+1}$represents the section (i, i+1) train running time, s. $t_{i,s}$ represents the train stopping time at station i, s; t_z represents the train operating time at the turnaround station, s. c_4 represents the cost of running the train per kilometre, yuan/km.

B. Restrictions

The constraints of the model are as follows.

$$f_{\min}\le f\le f_{\max} \tag{23}$$

$$1\le s_1\le s_2\le N \tag{24}$$

$$\eta_{i,i+1}^{\phi}\le\eta_{\max} \tag{25}$$

$$N_y\le N_{\max} \tag{26}$$

$$s_1,s_2,f\in Z^{+} \tag{27}$$

Where, (23) presents that the operation frequencies during the study period are limited between the minimum frequencies f_{min} and the maximum frequencies f_{max}. (24) presents the location of the turnaround stations s_1 and s_2 is in a reasonable interval. (25) presents that in order to make the journey more comfortable for passengers and improve the quality of metro service, the full train load ratio $\eta_{i,i+1}^{\phi}$ is limited to less than η_{max} for each section of the up and down trains. (26) presents that due to constraints such as the purchase cost and vehicle section equipment, the number of vehicles in operation N_y that can be put into service is limited to less than the maximum number of cars in use N_{max}. (27) presents an integer constraint on the decision variables.

IV. Algorithm Design

Quantum Genetic Algorithm (QGA) [29] effectively combines quantum computing-related theories with genetic algorithms. It has the advantages of fast convergence speed and the advantage of jumping out of locally optimal solutions. Non-dominated sorting genetic algorithm II (NSGA-II) is one of the most effective algorithms for solving multi-objective programming problems by introducing a fast non-dominated sorting algorithm and the crowded-comparison operator [30]. Since the model in this paper is nonlinear multi-objective programming [31], there is no suitable algorithm to find an exact solution. Therefore, based on the QGA and NSGA-II algorithms, we introduce the fast non-dominated sorting algorithm and the crowded-comparison operator in the NSGA-II algorithm into the QGA algorithm. An improved quantum genetic algorithm (IQGA) is proposed to solve multi-objective programming problems.

A. Quantum Encoding and Decoding

Since the decision variables in this paper include two positions of turnaround stations s_1, s_2 and operation frequencies f, a three-stage qubit encoding method is adopted. Compared with binary encoding, using this encoding method, a qubit not only represents two states of 0 or 1, but also represents any intermediate state between these two states [32], which increases the randomness of the population.

With qubit encoding, a qubit may be in $|1\rangle$ or $|0\rangle$, or in an intermediate state between $|1\rangle$ and $|0\rangle$, that is, different superposition states of $|1\rangle$ and $|0\rangle$, so a qubit state can be expressed as (28).

$$|\varphi\rangle=\alpha\,|0\rangle+\beta\,|1\rangle \tag{28}$$

Where, α and β can be complex numbers, representing the

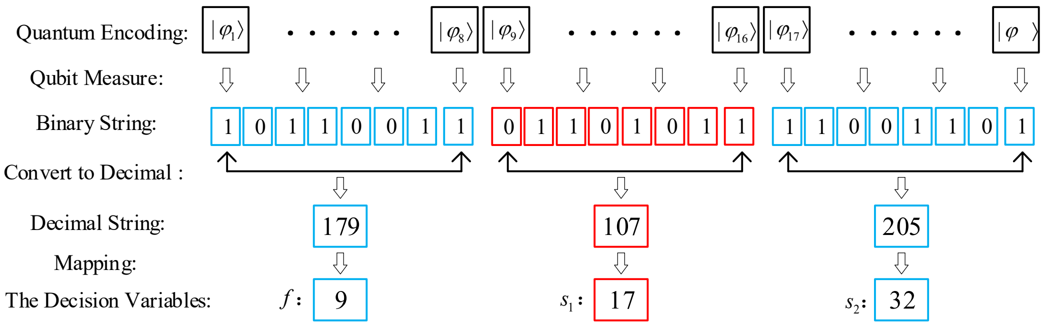

Fig.4 Schematic diagram of the decoding process

probability amplitude of the corresponding state and satisfying the normalization condition:

$$|\alpha|^2+|\beta|^2=1 \tag{29}$$

Where, $|\alpha|^2$ represents the probability of $|0\rangle$, and $|\beta|^2$ represents the probability of $|1\rangle$.

Based on the above properties, the specific encoding is shown in (30). The chromosome has a total of 3m qubits, which are divided into three segments of length m, respectively expressed as the turnaround stations s_1, s_2 and the operation frequencies f.

$$Q=\begin{bmatrix}\alpha_i\\ \beta_i\end{bmatrix}=\begin{bmatrix}\underbrace{\begin{matrix}\alpha_{1,1} \dots \alpha_{1,\ m}\\ \beta_{2,1} \quad \beta_{2,\ m}\end{matrix}}_{\text{code-}s_1}\ \underbrace{\begin{matrix}\alpha_{1,\ m+1} \dots \alpha_{1,\ 2m}\\ \beta_{2,\ m+1} \quad \beta_{1,\ 2m}\end{matrix}}_{\text{code-}s_2}\ \underbrace{\begin{matrix}\alpha_{1,\ 2m+1} \dots \alpha_{1,\ 3m}\\ \beta_{2,2m+1} \quad \beta_{2,\ 3m}\end{matrix}}_{\text{code-}f}\end{bmatrix} \tag{30}$$

A qubit-encoded chromosome can obtain a binary string through qubit measure, then decode the binary string into a decimal string according to each m bit from left to right as a chromosome segment, and then decode the decoding using the mapping method shown in (31). The resulting decimal string is mapped to the range of the decision variables, resulting in the actual values of the decision variables s_1, s_2,and f.

$$x_{ac}=\left[\frac{x_{ac}^{\max}-x_{ac}^{\min}}{x_{de}^{\max}}\right]\times x_{de}+x_{ac}^{\min} \tag{31}$$

Where, x_{ac} represents the actual value of the decision variable after decoding, $x_{ac}^{\min}$ and $x_{ac}^{\max}$ represent the upper and lower limits of the independent variable respectively, $x_{de}^{\max}$ represents the maximum value after the binary string is decoded into a decimal value, x_{de} represents the actual value after the binary string is decoded into a decimal value.

For example, the decoding process of a chromosome containing three decision variables is shown in Fig.4. As shown in Fig.4, suppose a quantum chromosome consists of three 8-bit-long chromosome segments encoding three decision variables. After quantum bit measurement, a binary string of 24 bits in length can be obtained. It can be decoded into three decimal numbers in groups of 8 bits from left to right. Then the range of decision variables is mapped by (31), which is the decoding process of quantum bit staining.

B. Quantum Rotation Gate

The quantum rotation gate is a specific measure for the quantum genetic algorithm to increase the diversity of the population [33]. An important Q-gate is the quantum rotation gate given by the rotation of the qubit by an angle $\Delta\theta$ in the Bloch sphere.

$$U=\begin{pmatrix}\cos\Delta\theta & -\sin\Delta\theta\\ \sin\Delta\theta & \cos\Delta\theta\end{pmatrix} \tag{32}$$

The new qubit is given by (33).

$$Q'=\begin{pmatrix}\alpha'\\ \beta'\end{pmatrix}=\begin{pmatrix}\cos\Delta\theta & -\sin\Delta\theta\\ \sin\Delta\theta & \cos\Delta\theta\end{pmatrix}\begin{pmatrix}\alpha\\ \beta\end{pmatrix} \tag{33}$$

Where, $(\alpha_i,\beta_i)^T$ and $(\alpha_i',\beta_i')^T$ are the probability amplitude before and after the update of the i-th qubit revolving gate of the chromosome; $\Delta\theta$ is the angle of rotation.

The operation strategy of the rotation angle $\Delta\theta$ directly affects the effect of the genetic algorithm. The rotation strategy adopted in this paper is shown in Tab.1.

TABLE I
QUANTUM GATE ROTATION UPDATE STRATEGY

X_i	X_{besti}	$f(x)\succ f(best_i)$	$\Delta\theta$	$s(\alpha_i,\beta_i)$: $\alpha_i\beta_i>0$	$\alpha_i\beta_i<0$	$\alpha_i=0$	$\beta_i=0$
0	1	FALSE	0	0	0	0	0
0	1	TRUE	0	0	0	0	0
0	1	FALSE	0.01 π	+1	-1	0	±1
0	1	TRUE	0.01 π	-1	+1	±1	0
1	0	FALSE	0.005 π	-1	+1	±1	0
1	0	TRUE	0.005 π	+1	-1	0	±1
1	0	FALSE	0	0	0	0	0
1	0	TRUE	0	0	0	0	0

In Tab.1, X_i is the i-th position of a current binary-coded individual. Because in the classical quantum genetic algorithm, the quantum revolving gate update strategy evolves toward the optimal individual X_{besti}, the solution is updated towards the Pareto solution, and the individual compromise solution X_{besti} in the Pareto solutions is selected as the update direction. $s(\alpha_i,\beta_i)$ indicates the direction of rotation, $f(x)\succ f(x_{besti})$ indicates that the individual x is dominated, if $f(x)\succ f(x_{besti})$, adjust the corresponding qubit of the current individual, so that the probability amplitude pair $(\alpha_i,\beta_i)^T$ evolves in the direction of X_i, otherwise, adjust the corresponding quantum bits of the current individual make the probability amplitude pair $(\alpha_i,\beta_i)^T$ evolve in the direction of X_{besti}.

C. Quantum Crossover and Quantum Mutation

In order to ensure the integrity of the population and speed up the convergence of the algorithm, this paper adds quantum crossover and quantum mutation operations based on the quantum gate update strategy. The crossover objects are qubits. The chromosome segments corresponding to each decision variable were subjected to single-point crossover and single-point variation, where the crossover and variation of one segment of the chromosome are shown in Fig 5.

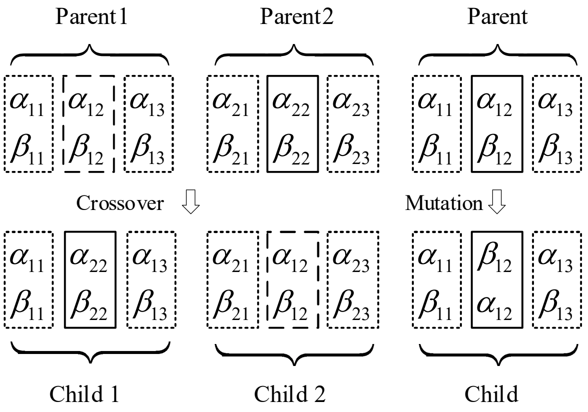

Fig.5. Schematic diagram of quantum crossover and mutation

In addition, in order to avoid the algorithm falling into the optimal local solution, we introduce an adaptive mutation probability and crossover probability, as shown in (34) and (35), when the evolution falls into the optimal local solution, the mutation probability becomes larger and new individual genes are added. And the ability to jump out of the optimal local solution ensures the global search ability of the algorithm.

$$p_c = \frac{0.99}{\exp(\frac{n_{count} \times n_{gen}}{n_{num}}) + 1} + 0.5 \tag{34}$$

$$p_{\mathrm{m}} = \frac{0.1}{\exp(-\frac{n_{count} \times n_{gen}}{n_{num}}) + 1} \tag{35}$$

Where, n_{gen} is the number of iterations of the population. n_{count} is the algebraic accumulation of the optimal value unchanged. n_{num} is the maximum number of iterations set. It can be seen from the formula that p_c and n_{gen} will be adaptively adjusted as n_{gen} and n_{count} change.

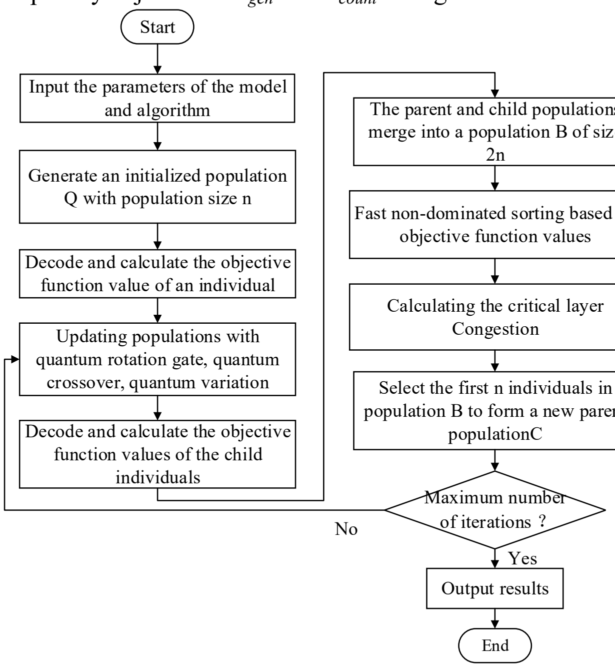

Fig.6. IQGA algorithm flowchart

D.Algorithm Flow

In the NSGA-II, a fast non-dominated sorting approach is the crucial operation to solve the multi-objective programming problem, and the crowded-comparison operator can keep the population diverse. Based on the operation of the quantum genetic algorithm, this paper adds the fast non-dominated sorting approach and the crowded comparison operator. The algorithm flowchart is shown in Fig.6.

V. CASE STUDY

A. Case Background

In order to verify the model and algorithm, taking a city metro line as an example, the line has a total of 41 stations, and the passenger flow data during 9:00 to 10:00 on weekdays are selected. The Cross-section passenger flow is shown in Fig.7, and the spatial distribution of passenger flow is atrophic distribution at both ends, so the train plan proposed in this paper can be adopted. The operating vehicles of this line adopt the vehicles that conform to the train coupling and uncoupling operation. The model parameters are shown in Tab.2.

TABLE II
MODEL PARAMETERS

Symbols	Meaning of the symbols	Numerical values		Unit
B	The average time value of a passenger	30		yuan/h
Q	Train capacity of the unit train	930		people/unit
n_1	The number of lamps in a single vehicle	40		unit
n_c	The number of vehicles of a train	Unit train	3	unit
		Reconnection train	6	unit
s_c	The surface area inside the vehicle	282.64		m^2
$\lvert T_i\text{-}T_o\rvert$	Temperature difference between inside and outside the vehicle	10		°C
m_1	The quality of unit train	38.8×3		t
m_2	The quality of a passenger	60		kg
G	Gravitational acceleration	9.81		m/s^2
V	The average train speed	35		km/h
v_{max}	the maximum operating speed	80		km/h
Γ	thermal power generation ratio	0.8		-
c_3	The unit train acquisition cost	18,000,000		yuan/unit
T_y	The number of hours converted from train service life	124,100		h
c_4	The cost of running the train per kilometer	8		yuan/h
c_5	The single coupling and uncoupling cost	200		yuan
f_{min}	The minimum frequencies	6		pairs /h
f_{max}	The maximum frequencies	10		pairs /h
η_{max}	The maximum full load rate of the train	120%		-

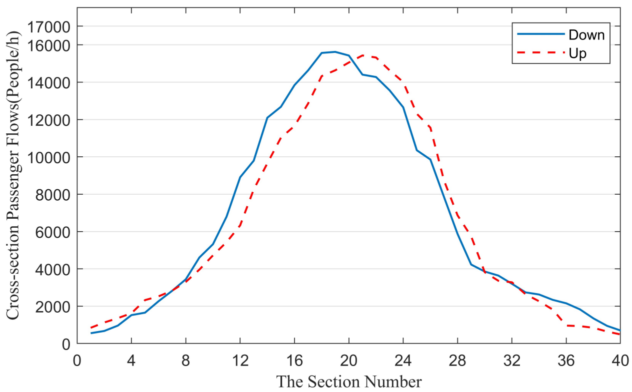

Fig.7. Cross-section passenger flows

B. Results Analysis

B.1. Algorithm Analysis

The above parameters are substituted into the model, based on the Matlab programming development environment, using the algorithm proposed in this paper. The algorithm parameters are set as follows: the population size is 200, and the number of iterations is set to 300. The Pareto solution set distribution obtained by the operation is shown in Fig.8.

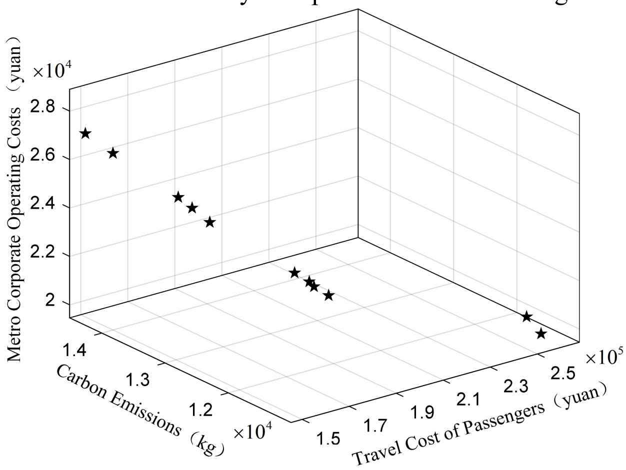

Fig.8. Pareto solution set

It can be seen from Fig.8 that the Pareto solution set contains 11 effective solutions, and the number is far fewer than the population size because the decision variables in this paper are all integers and the numerical range is small. From the side analysis, the algorithm has good applicability to this mathematical model.

To verify the superiority of IQGA to the multi-objective programming model in this paper, the NSGA-Ⅱ algorithm was used to solve the problem with the same population size and iteration times. The crossover probability was set as 0.8 and the mutation probability to 0.1. The mean values of the three objective functions of the individuals in the population were selected as the reference objects respectively, and the iterative plots of the three objective functions were obtained as shown in Fig.9,10, and 11.

As shown in Fig.9,10, and 11, IQGA and NSGA-II are consistent in their results. Nevertheless, IQGA converges at about the 36th generation while NSGA-II converges at about the 44th generation. It can be verified that IQGA effectively solves multi-objective programming models and has the advantages of faster convergence and stable operation.

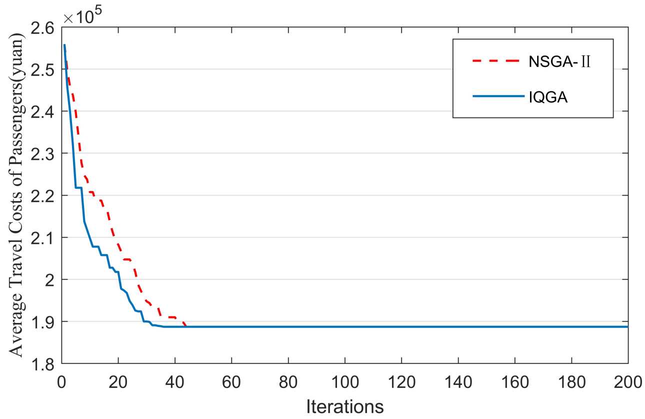

Fig.9. Algorithm iteration graph of average travel cost of passengers

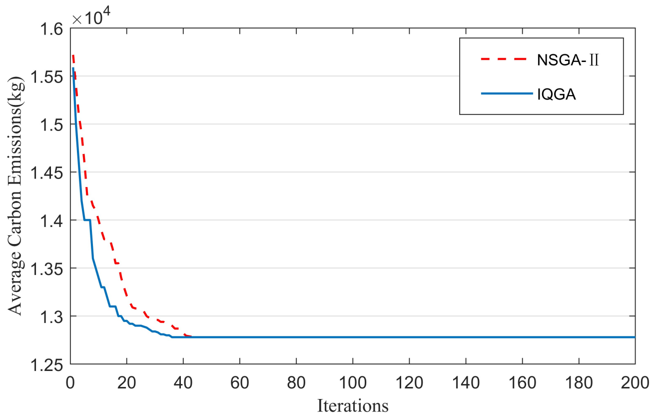

Fig.10. Algorithm iteration graph of average carbon emission

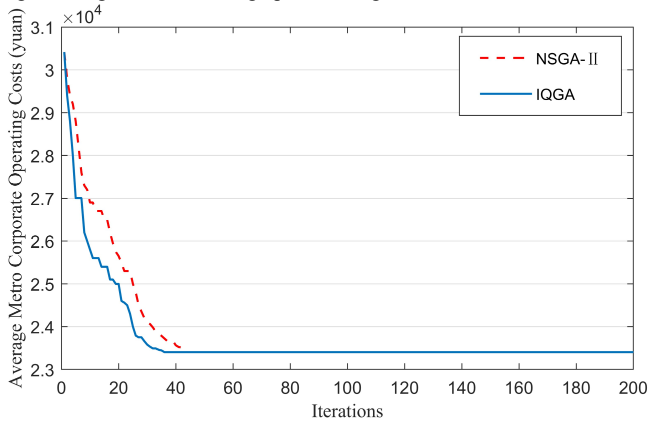

Fig.11. Algorithm iteration graph of average metro corporate operating costs

B.2. Optimal Train Plan

The set of Pareto solutions in Fig.8 selected as the optimal train plans for this model is shown in Tab.3.

TABLE III
THE SET OF OPTIMAL TRAIN PLAN

No.	f (pairs /h)	s_1	s_2	Travel cost of passengers (yuan)	Carbon emission (kg)	Metro corporate operating costs (yuan)
1	10	14	27	149268.00	14409.11	27087.85
2	10	14	26	154140.58	14153.64	26457.62
3	9	12	27	165853.33	13557.11	25059.71
4	9	13	27	167241.32	13389.58	24787.45
5	9	14	27	169476.13	13193.26	24379.06
6	8	12	28	186585.00	12488.14	22698.81
7	8	13	28	188808.29	12339.22	22456.80
8	8	12	27	189789.81	12300.83	22275.30
9	8	13	27	192013.10	12151.92	22033.29
10	7	12	29	255925.78	11398.47	20355.56
11	7	12	28	256957.79	11208.45	19861.46

As can be seen from Tab.3, under the line conditions and passenger flow conditions in the case, the operation frequencies of TPFTC range between 7 pairs/h and 10 pairs/h, and the location of the turnaround stations is at the excessive position of the transition from high to low passenger flow in the section.

VI. Results Analysis

A. Comparison of the Objective Functions between TPFTC and TTP

To verify the advantages of TPFTC, four train plans with different operation frequencies in the Pareto solution are selected to compare with the TTP. Four train plans are {7, 12, 29}, {8, 12, 28}, {9, 12, 27}, and {10, 14, 27}. Since the travel costs of passengers of the four train plans are the same, the comparison of carbon emission and metro corporate operating costs are shown in Fig.12 and 13.

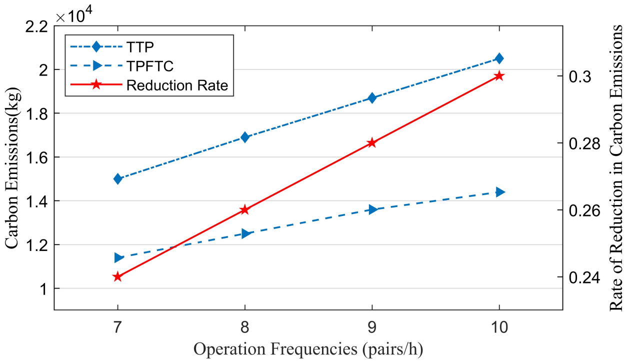

Fig.12. Schematic diagram of carbon emission comparison between TPFTC and TTP

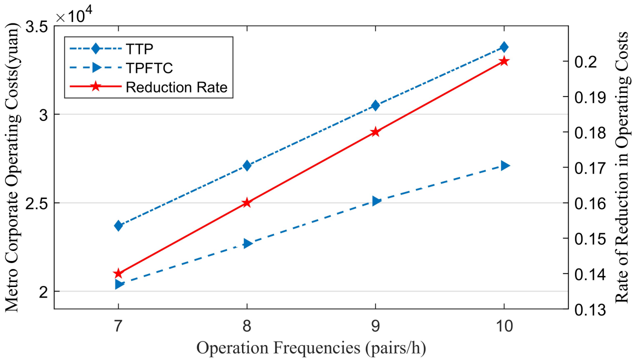

Fig.13. Schematic diagram of metro corporate operating costs comparison between TPFTC and TTP

The travel costs of the passenger under TTP and TPFTC are the same in the four selected train plans. In the actual operation process, it means that under these two plans, the waiting time of passengers and the degree of traffic congestion remain unchanged. At the same time, carbon emission and metro corporate operating costs have been significantly reduced. As shown in Fig.12 and 13, under the condition that the passenger travel costs of the passenger remain unchanged when the operation frequencies are 7 pairs/h, 8 pairs/h, 9 pairs/h, and 10 pairs/h respectively, the carbon emission is reduced by 24.26%, 26%, 27.52%, and 29.83%, and the metro corporate operating costs are reduced by 14.09%, 16.18%, 17.74%, and 19.98% respectively. The reason is that the TPFTC reduces the number of vehicles put into operation because the unit trains run in the section with small passenger flow demand. However, the unit train group can already meet the small passenger flow, so the service intensity is not changed.

In summary, TPFTC significantly reduces carbon emission and metro corporate operating costs without increasing passenger travel costs, indicating that TPFTC is conducive to energy saving and emission reduction under the condition that the passenger flow is atrophic distribution at both ends.

B. Comparison of the Full Load Rate of the Train between TPFTC and TTP

The full load rate of the train of the TPFTC and TTP are compared in the M_1 and M_3 sections as shown in Fig. 14 and 15 .

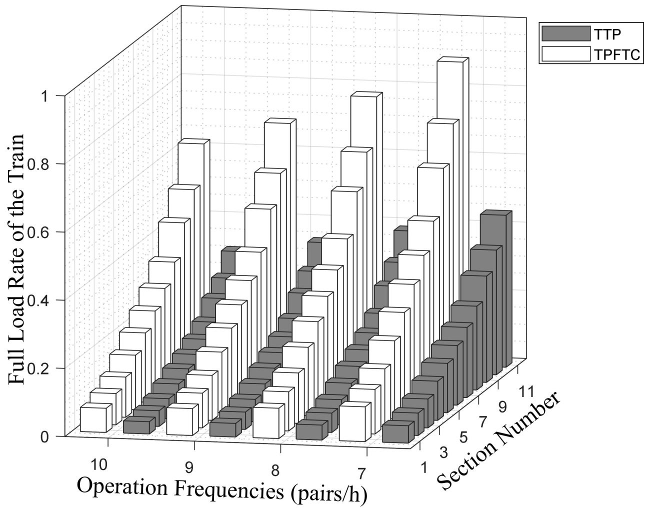

Fig.14. Schematic diagram of the full load rate of the train in M_1 between TPFTC and TTP

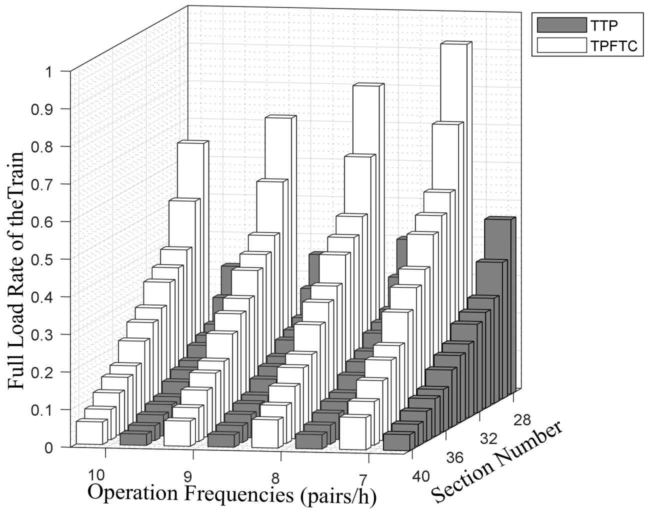

Fig.15. Schematic diagram of the full load rate of the train in M_3 between TPFTC and TTP

As shown in Fig.14 and 15, compared with TTP, in sections M_1 and M_3 with smaller cross-section passenger flow, the cross-section full load rate is doubled, and the full load rate of the train in the improved cross-section does not exceed 100%. It shows that increasing the full load rate does not reduce the operators' service quality. It is also the key to reducing operating costs and carbon emission in TPFTC without increasing passengers' travel costs. The comparison charts of the average full load rate of the line under TPFTC and TTP in the up and down directions are shown in Fig.16 and 17.

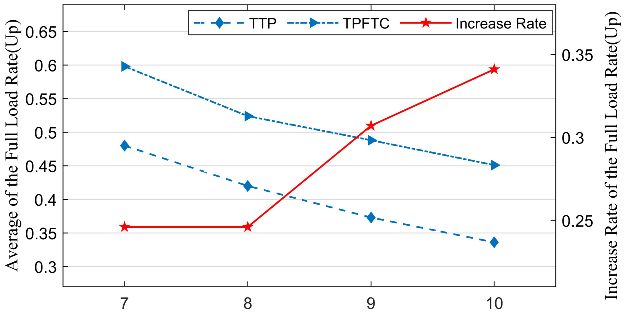

Fig.16. Comparison of the average full load rate of the line in the up direction

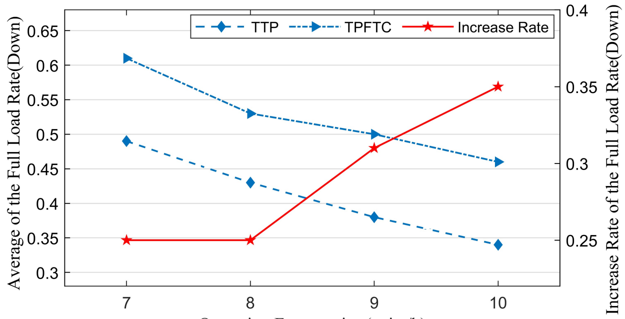

Fig.17. Comparison of the average full load rate of the line in the down direction

As shown in Fig.16 and 17, the average full load rate of TPFTC is higher than TTP during the study period. When the operation frequencies are 7 pairs/h, 8 pairs/h, 9 pairs/h, and 10 pairs/h respectively, the average full load rate of the whole line increases by 25%, 25%, 31%,and 35% respectively in the up direction, and 25%, 25%, 30%,and 34% respectively in the down direction. The average full load rate gradually decreases as the operation frequencies increase, but the higher the operation frequencies, the higher the increase rate of the average full load rate increases. It indicates that the higher the operation frequencies, the more pronounced the advantage of TPFTC.

C. Sensitivity Analysis of Locations of Turnaround Stations

A frequency of 10 pairs/h was chosen to analyse the change in the objective function and the full load rate under different turnaround plans, where the turnaround plans on the objective function change as shown in Fig.18 and the average full load rate of the line change as shown in Fig.19.

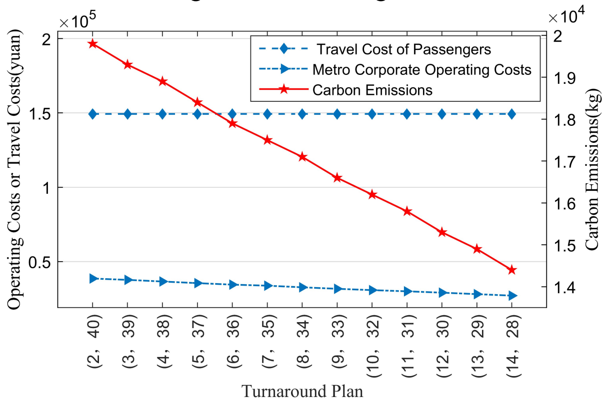

Fig.18. Schematic diagram of the effect of the turnaround plan on the objective functions

As seen from Fig.18, with the location of the turnaround stations closer, the cost of passenger travel remains the same, while carbon emissions are reduced by 5,826.19 kg and metro corporate operating costs are reduced by 12,528.96 yuan.

The reason is that the operation frequencies are not changed, and each section does not cause congestion, so the passenger travel cost remains unchanged. The shorter the distance of section M_2, the shorter the travel distance of the reconnection train, and the longer the travel distance of the unit train, so the carbon emission and metro corporate operating costs are less in the same period. The above reasons are also the key to the obvious advantages of TPFTC.

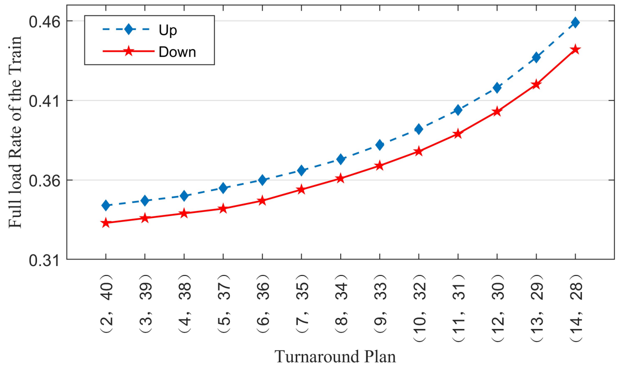

Fig.19. Schematic diagram of the effect of the turnaround plan on the full load rate of the line

As can be seen from Fig.19, the average full load rate of the metro line does not exceed 0.5 even when the distance of the reconnecting composition section M_2 is short. To meet the passenger demand in the critical section, resulting in a waste of transportation capacity in the subway section. While the current subway operation mode is mainly TTP, metro operating companies should actively adopt more flexible operation modes such as TPFTC.

The maximum full load rate of metro trains η_{max} will vary depending on line conditions, passenger flow conditions, etc. Different maximum full load rates will change the turnaround stations' location, impacting metro corporate operating costs and carbon emissions. Assuming the operation frequencies are 10 pairs/h, as the η_{max} is between 1 and 1.8, the change of the optimal turnaround stations is shown in Tab.4.

TABLE IV
SENSITIVITY ANALYSIS OF THE MAXIMUM FULL LOAD RATE

	f (pairs /h)	7	8	9	10
	Turnaround Stations	(s_1,s_2)	(s_1,s_2)	(s_1,s_2)	(s_1,s_2)
η_{max}	1.0	(- , -)	(12 , 28)	(12 , 27)	(14 , 27)
	1.1	(- , -)	(12 , 28)	(13 , 27)	(14 , 27)
	1.2	(12 , 28)	(13 , 27)	(14 , 27)	(14 , 26)
	1.3	(13 , 28)	(14 , 27)	(14 , 27)	(15 , 26)
	1.4	(13 , 27)	(14 , 27)	(15 , 26)	(15 , 25)
	1.5	(14 , 27)	(14 , 26)	(15 , 26)	(15 , 25)
	1.6	(14 , 27)	(15 , 25)	(15, 26)	(15 , 25)
	1.7	(14 , 26)	(15 , 25)	(15 , 26)	(15 , 25)
	1.8	(15 , 25)	(15 , 25)	(15 , 26)	(15 , 25)

As shown in Tab.4, as the maximum full load of the train increases, the closer the location of the turnaround station is. Therefore, the higher the maximum full load rate, the shorter the distance traveled by the reconnection train, the less the operating costs and carbon emissions. However, this situation also causes train congestion, which is the purpose of energy saving and emission reduction with reduced service quality of the metro operating company.

D.Sensitivity Analysis of the Number of Train Compositions

Compared with TTP, the operation frequencies of TPFTC are limited by the operation time of the coupling and decoupling operations at turnaround stations. Therefore, when the passenger flow in some sections is more numerous than the maximum transportation supply capacity, increasing the number of vehicles in the unit train can improve service quality. Based on this, it is necessary to analyse the relationship between the number of vehicles and passenger flow. When the number of vehicles in the unit train is different, the maximum conveying capacity of the section is different. The sensitivity analysis diagram of the number of vehicles per train is shown in Fig.20.

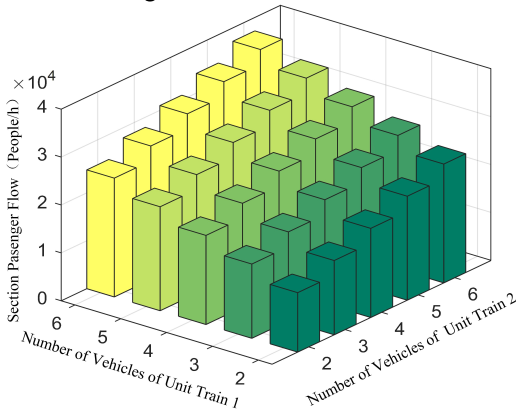

Fig.20. Sensitivity analysis of the number of train compositions

As shown in Fig.20, the maximum conveying capacity of the reconnection section varies with the number of vehicles in the unit train. The number of vehicles in the unit train can be determined according to the passenger flow of different sections. Under the limitation, if the transportation demand cannot be met at the maximum composition. It means that TPFTC is unsuitable for this line, and TTP should be used to increase the operation frequencies to meet the transportation demand.

In addition, under the specific passenger flow, the carbon emission during the operation of the subway will change with the different number of unit train 1 and unit train 2, and the change of carbon emission of the subway with the number of unit train compositions is shown in Fig. 21.

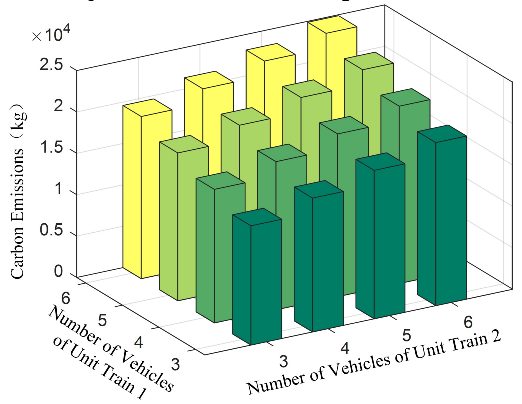

Fig.21. Sensitivity analysis of the number of train compositions about carbon emission

As shown in Fig.21, the carbon emissions increase from 14409.11kg to 24882.6kg when the number of unit train 1 and unit train 2 increases from 3 to 6 under a specific passenger flow. Compared with the minimum number of unit trains, the carbon emission growth rate is 72.7% when the number of unit trains 1 and 2 is six. Therefore, choosing more matching unit trains according to the passenger flow of different sections is extremely effective to save energy and reduce emissions.

VII. Conclusions

The following conclusions can be drawn from the case study.

(1) TPFTC does not reduce the service level of the metro, and the comfort level of passengers during the journey is same as TTP. However, at the same service level, when the operation frequencies are 7 pairs/h, 8 pairs/h, 9 pairs/h, and 10 pairs/h, the carbon emission reduces by 24.26%, 26%, 27.52%, and 29.83%, and the metro corporate operating costs reduce 14.09%, 16.18%, 17.74%, and 19.98% respectively. TPFTC is effective for energy saving and emission reduction during metro operation.

(2) TPFTC can significantly increase the average full load rate of the line. In addition, the average full load rate gradually decreases with the increase of the frequencies. However, the higher the frequencies, the higher the average full load rate increases. It indicates that the higher the frequencies, the more pronounced the advantage of TPFTC.

(3) Carbon emission and metro corporate operating costs are related to the location of the turnaround stations. The closer the location of the turnaround stations, the higher the average full load rate of the line section, so the carbon emission and metro corporate operating costs are smaller. And the higher the maximum full load rate, the closer the location of the turnaround stations, which is conducive to energy saving and emission reduction, but it will reduce the comfort of passengers during the journey.

(4) The operation frequencies of TPFTC are limited due to the effect of the coupling and uncoupling operation and turnaround operation. If the transport demand cannot be met when the maximum number of compositions is operated, it means that the mode is not applicable to the line conditions. Furthermore, according to the passenger flow, the flexible choice of unit trains can significantly reduce carbon emission to achieve the purpose of energy saving and emission reduction.

(5) In terms of algorithm, the IQGA can effectively solve multi-objective programming problems and has excellent performance because of its quantum bit encoding and quantum revolving gate strategy, which makes the algorithm conducive to jumping out of local optimum solutions and iterative stability.

Under the suitable passenger flow conditions, the advantages of the TPFTC are obvious, so the train timetabling and rolling stock circulation planning with flexible train composition will be the focus of the next study.

REFERENCES

[1] B.Y. Xu,T.J. Wang,D.Y. Ma,R. Song,M. Zhang, "Impacts of regional emission reduction and global climate change on air quality and temperature to attain carbon neutrality in China," *Atmospheric Research*, vol.279, Article ID. 106384,2022.

[2] M. Meinshausen, S. J. Smith, K. Calvin, J. S. Daniel, M. L. T. Kainuma, J. F. Lamarque, et al, "The RCP greenhouse gas concentrations and their extensions from 1765 to 2300," *Climatic Change*, vol.109 ,pp. 213-241,2011.

[3] S. Su, T. Tang, Y.H. Wang, "Evaluation of strategies to reducing traction energy consumption of metro systems using an optimal train control simulation model," *Energies*, vol.105,no.9,pp. 1-19,2016.

[4] L.Y. Meng, and X.S. Zhou, "An integrated train service plan optimization model with variable demand: a team-based scheduling approach with dual cost information in a layered network," *Transportation Research Part B: Methodological*, vol. 125, pp. 1 –28, 2019.

[5] M. Nold, and F. Corman, "Dynamic train unit coupling and decoupling at cruising speed: Systematic classification, operational potentials, and research agenda," *Journal of Rail Transport Planning & Management*, vol. 18, Article ID. 100241,2021.

[6] H.C. Pan,L.X. Yang,Z. Liang, "Demand-oriented integration optimization of train timetabling and rolling stock circulation planning with flexible train compositions: A column-generation-based approach," *European Journal of Operational Research*,2022.DOI: https://doi.org/10.1016/j.ejor.2022.05.039

[7] Y. Sun,Q.Z. Shi,Y. Zhao,Q.Y. Kong, "Method on making train running plan for urban railway traffic," *Journal of Tongji University (Nature Science)*, vol. 32, no.8,pp. 1005-1014,2004.

[8] H.M. Niu,M,M. Chen,M.H. Zhang, "Optimization theory and method of train operation scheme for urban rail transit," *China Railway Science*, vol. 32, no.4,pp. 128-133,2011.

[9] Y.T. Zhu,B.H. Mao,Y. Bai,S.K. Chen, "Bi-level model for single-line rail timetable design with consideration of demand and capacity," *Transportation Research Part C: Emerging Technologies*, vol. 85, pp. 211-233,2017.

[10] C.J. Dai,Y.Z. Li,Z.S. Zhan,H. Chai, "Optimization of train operation scheme for urban rail transit considering dynamic passenger demand and full-length & short-turn routing modes," China Railway Science, vol.39, no.2,pp. 128-136,2018.

[11] H. Niu and M. Zhang, "An optimization to schedule train operations with phase-regular framework for intercity rail lines," *Discrete Dynamics in Nature and Society*, vol. 2012, Article ID. 549374,2012.

[12] D.D. Yu,B.M. Han,Q. Zhang,X.M. Yao,F.L. Liu, "Optimization method for train plan of urban rail transit based on the flexible length of train formation," Journay of Beijing Jiaotong University, vol.39, no.6,pp. 21-31,2015.

[13] Y.P. Rong,X.C. Zhang,Y. Bai,D.J. Xu, "Optimization for Train Plan of Urban Rail Transit Based on Hybrid Train Formation," *Journal of Transportation Systems Engineering and Information Technology*, vol.16, no.5,pp. 117-122,2016.

[14] Z. Cao, A. Ceder, D. Li, S. Zhang, "Robust and optimized urban rail timetabling using a marshaling plan and skip-stop operation," Transportmetrica A: Transportation Science, vol. 16, no. 3, pp. 1217–1249, 2020.

[15] Z.Y. Li, J. Zhao, Q.Y. Peng, "Train service design in an urban rail transit line incorporating multiple service routes and multiple train compositions," *Transportation Research Part C: Emerging Technologies*,vol.123,Article ID. 102959,2021.

[16] Z.Y. Li,J. Zhao,Q.Y. Peng, "Optimizing the train service route plan in an urban rail transit line with multiple service routes and multiple train sizes," *Journal of the China Rail Way Society*, vol. 42, no. 6, pp. 1-11, 2020.

[17] D.J. Xu,B.H. Mao,S.K. Chen,L. Gong,J.W. Zeng, "Optimization of operation scheme for ful-length and short turn routings considering operation proportion," *Journal of Traffic and Transportation Engineering*, vol. 21, no. 2, pp. 173-186, 2021.

[18] Q.W. Zeng ,and Q.Y. Peng, "Study on the cross-line train plan in urban rail transit considering the multi-group train," *Journal of Railway Science and Engineering*,2022.DOI: https://doi.org/10.19713/j.cnki.43-1423/u.T20220780

[19] A.A. Yang,J.Y. Sun,B. Wang,S.K. Chen,W. Ming, "Optimization of virtual-coupling-orientated train operation plan based on full-length and short-turn routing," *Journal of Beijing Jiaotong University*, vol. 46, no. 4, pp. 9-14, 2022.

[20] H.S. Zhou,J.G. Qi,L.X. Yang,J.G. Shi,C.C. Gong, "Joint optimization for rolling stock circulation plan based on flexible train composition mode and robust passenger flow control strategy on urban rail transit lines," *Control and Decision*,2022.DOI: https://doi.org/10.13195/j.kzyjc.2021.2054

[21] H.S. Zhou,J.G. Qi,L.X. Yang,J.G. Shi,H.C. Pan,Y. Gao, "Joint optimization of train timetabling and rolling stock circulation planning: A novel flexible train composition mode," *Transportation Research Part B: Methodological*, vol.162, pp. 352-385, 2022.

[22] Y.Y. Yin,J. Chen,W.R. Zhao, "Collaborative optimization of passenger control strategy and train operation plan with variable formations for a rail transit network," *Journal of Advanced Transportation*, vol.2022 ,Article ID. 1647306,2022.

[23] X.C. Ran, S.K. Chen, L. Chen, W.Z. Jia, "An energy-efficient timetable optimization method for metro operation considering spatial distribution of passenger flow," Journal of Transportation Systems Engineering and Information Technology, vol. 30, no. 2, pp. 103-110, 2020.

[24] L.B. Deng,Q. Zeng,W. Gao,W.L. Zhou, "Research on train plan of urban rail transit with elastic demand," *Journal of the China Rail Way Society*, vol. 34, no. 12, pp. 16-25, 2012.

[25] J.Y. Long,Y. Li,L. Ma, "Research on carbon emission calculation in the process of urban rail transit," *Journal of Guiyang Cpllege(Natural Sciences)*, vol. 6, no. 2, pp. 1-11, 2012.

[26] X.B. Zheng,Y. Bai,S.S. Zhou, "Metro train energy consumption characteristics based on empirical data analysis," *Journal of Transportation Systems Engineering and Information Technology*, vol. 21, no. 6, pp. 264-271, 2021.

[27] J.Q. Ma,Y. Bai,B.M. Han, "Characteristic analysis of basic unit and complex network for urban rail transit," *Journal of Traffic and Transportation Engineering*, vol.10, no. 4, pp. 264-271, 2010.

[28] Y.Z. Dai,S. Zhang, "Analysis of full-length and short-turn routing of urban rail transit considering carbon emission," *Journal of Railway Science and Engineering*,2022.DOI: https://doi.org/10.19713/j.cnki.43-1423/u.T20220149

[29] K.H. Han,J.H. Kim, "Quantum-inspired evolutionary algorithm for a class of combinatorial optimization," *IEEE Transactions on Evolutionary Computation*, vol.6, no. 6, pp. 580-593, 2002.

[30] L.N. Wang， C.K.P. Zhang, "Greenhouse Microclimate Control Strategy to Reduce Costs Based on Improved NSGA-II Optimal Method," *Engineering Letters*, vol.29, no.3, pp. 818-823, 2021.

[31] L.X. Dang,Y.E. Hou,Q.S. Liu,Y.F. Kong, "A Hybrid Metaheuristic Algorithm for the Bi-objective School Bus Routing Problem," *IAENG International Journal of Computer Science*, vol.46, no.3, pp. 409-416, 2019.

[32] X.B. Liu,X. Jiao,T. Ning,X. Liang, "Flexible job shop scheduling based on double chains quantum genetic algorithm," *Computer Integrated Manufacturing Systems*, vol.21, no. 2, pp. 495-502, 2015.

[33] Y. Rubio,C. Olvera,O. Montiel, "Quantum-Inspired Evolutionary Algorithms on IBM Quantum Experience," *Engineering Letters*, vol.29, no.4, pp. 1573-1584, 2021.

Changfeng Zhu was born in Gansu, China , in 1972. In 2003 and 2013, he obtained master's and doctor's degrees in the Planning and Management of Traffic and Transportation in Lanzhou Jiaotong University. He is now a professor and doctoral supervisor of the School of Traffic and Transportation of Lanzhou Jiaotong University. His main research direction is transportation planning and management. He has made fruitful research achievements, presided over a number of national and local level fund projects, and published more than 30 papers that were retrieved by databases EI and SCI.